

Electron excitation of Li *S* and *D* states

A. Zajonc* and Alan Gallagher†

Joint Institute for Laboratory Astrophysics, University of Colorado and National Bureau of Standards, Boulder, Colorado 80309

(Received 18 May 1979)

Electron-impact excitation of the Li *3S*, *4S*, *3D*, and *4D* states have been measured from threshold to 1200-eV impact energy. The intensities of emission lines from these states have been measured relative to the *2P-2S* resonance line, and cross sections are obtained by normalizing to the resonance-line cross section and correcting for branching ratios. Cascade corrections to these total cross sections have been made at the higher energies, using available Born cross sections. The resulting direct cross sections show a uniform convergence at high energy to available Born cross sections and to E^{-1} behavior. At lower energies the *S*- and *D*-state cross sections have very different forms: the *S* states rise abruptly at threshold and drop rapidly past a narrow peak, while the *D* states rise gradually to a very broad maximum. Comparisons are made to available cross section calculations.

INTRODUCTION

The alkali-metal atoms offer particularly simple tests of electron collision processes; the wave functions and coupling schemes are simple, there are no degeneracies as in H, and their properties vary smoothly with increasing mass. Electron-alkali-atom collisions are also important in a variety of devices, such as metal vapor lamps and magnetohydrodynamic generators. Although electron excitation of alkali atoms have been measured many times since as early as the 1920s, there are many contradictions and gaps in the data. In recent years a very large number of these cross sections have been measured by Zapetschnyi and collaborators,^{1,2} while measurements in our laboratory have obtained the resonance-line cross sections.^{3,4}

By carefully measuring the energy dependence of the resonance-line excitation functions to high energy, where they can be reliably normalized to the Born cross section, we believe that we have been able to obtain the resonance-line cross sections in previous measurements^{3,4} with an accuracy of better than 5%. In the present measurements we took advantage of this by normalizing the higher-state excitations to the resonance-line cross section. Thus we have measured the intensity of the line emission from several excited states of Li relative to the resonance-line intensity. The intensity of lines from the higher states were much weaker, of course, so that it was often necessary to count photons for several minutes at a time and to be careful of spurious light leakage, background-gas signals, etc. The use of an efficient optical system helped considerably in this regard, as it was possible to work with low Li-beam density and electron-beam current and still have enough signal to check out possible sources of error.

There have been many calculations of alkali-

atom resonance-line excitation cross sections, but relatively few for the higher-state cross sections. Born-approximation cross sections are available for essentially all cases,^{5,6} providing interesting comparisons to the high-energy behavior reported here. Less approximate calculations that include higher excited states are understandably rare, and only two exist for the Li states studied here.^{7,8}

EXPERIMENT

The apparatus used for these measurements has been described in detail previously,^{3,4} and we will give only a brief outline here. A Li beam, typically of $\sim 10^{10}$ cm⁻³ density, is crossed by an electron beam and the line emission in the third, orthogonal direction is detected. Electron-beam currents are maintained well below space-charge-limited conditions, typically at ~ 50 μ A at 100 eV and ~ 0.5 μ A at 4 eV, and considerable care is taken to ensure that essentially all electrons traverse the observed portion of the atom beam and are collected. The oxide cathode yields an energy resolution of about 0.25 eV full width at half maximum (FWHM). The line emission is collected with $f:2$ optics, filtered with interference filters, detected with a dry-ice-cooled GaAs-type photomultiplier, and photon counted. Typical photon counting rates are 10^4 sec⁻¹ for the resonance line and 10^2 sec⁻¹ for the other lines at 100 eV. For these relatively weak emissions from the higher states, considerable care and testing was done to be certain that other Li lines or background-gas bands were not contributing to the observed signals. Since these *S-S* and *S-D* excitations fall off as E^{-1} at high energy, while some background-gas lines fall off less rapidly ($E^{-1}\log E$) such leakage was particularly troublesome at high energy, sometimes yielding as much as 30% of the total signals. (Typical background-gas

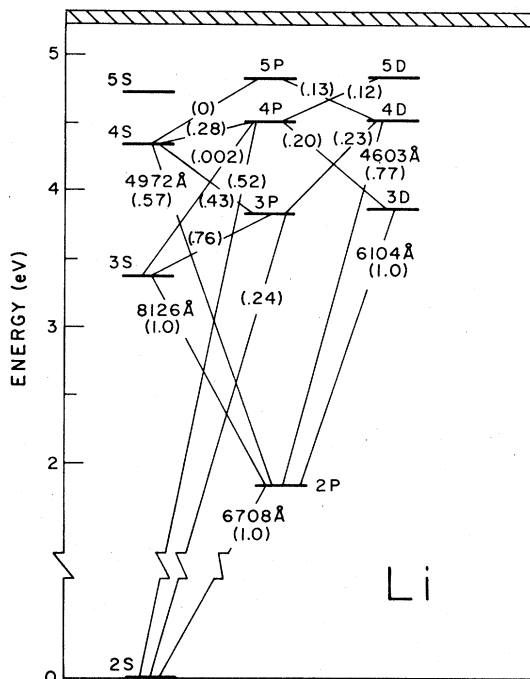


FIG. 1. Energy-level diagram for Li. The wavelengths of the detected lines are given, and the branching ratios for these and the principal cascading lines are shown.

pressure was $\sim 10^{-8}$ Torr.) To discriminate against background gas, oven light, etc., the difference in photon counting rates with the Li-beam stop open and shut was recorded. (No effect of this beam stop on light levels was detectable with the electron beam off.) Possible leakage of the Li resonance line through the other filters was checked and found to be negligible.

The S- and D-state emission lines studied here have wavelengths between 413.3 and 812.6 nm, while the resonance line is at 670.8 nm (see Fig. 1). The interference-filter transmissions were accurately measured by observing their attenuation of the appropriate Li line, filtered from a Li hollow-cathode lamp. The experimental optics utilized two quartz lenses and two achromatic glass lenses. The quartz lenses have slightly different focal properties at the different wavelengths, but tests of intensity ratios for various lens positions indicated that this caused less than 3% uncertainty in relative sensitivity even for the most extreme wavelengths. From manufacturers' specifications the photomultiplier quantum efficiency is supposed to vary smoothly and by about a factor of 1.7 between 400 and 800 nm. It was assumed that this represents the sensitivity variation of the entire optical detection system; the fact that we have not checked this with a direct calibration is the major uncertainty in the magnitudes of the reported cross sections.

RESULTS

The intensity ratios of the resonance versus higher-state lines were measured at a variety of Li-beam densities, background-gas densities, and electron-impact energies to test for systematic effects. Based on the results of these tests, we believe that the ratios of the reported cross sections at low versus high energies (e.g., 7 vs. 1000 eV) are accurate to $\sim 5\%$ for the 3S and 3D states and to $\sim 10\%$ for the weaker 4S- and 4D- state emissions. The absolute values of the reported cross sections contain the additional uncertainty in optical detection efficiency relative to that at 670.8 nm. This is estimated at 5% for the 3D state (610.4 nm), and 10% for the 3S (812.6 nm), 4D (460.3 nm), and 5S (497.2 nm) states.

The photomultiplier counting rate $S(i, \lambda)$ for the line λ from state i is related to the total excitation cross section Q_i by

$$S(i, \lambda) = K(\lambda) \Delta\Omega D(\lambda) T(\lambda) B(i, \lambda) \left(1 - \frac{1}{3} P_{i\lambda}\right)^{-1} Q_i. \quad (1)$$

Here $K(\lambda)$ is the transmission and $\Delta\Omega$ the solid angle of the collection optics, $D(\lambda)$ is the photomultiplier quantum efficiency, $T(\lambda)$ is the interference-filter transmission, and $B(i, \lambda)$ is the branching ratio for state i into line λ . Since we detect the emission at 90° to the electron beam, the anisotropy correction $1 - \frac{1}{3} P_{i\lambda}$ is necessary, where $P_{i\lambda}$ is the polarization of the emission of wavelength λ from state i . From Ref. 9, we have used $B(3S, 812.6 \text{ nm}) = 1$, $B(3D, 610.4 \text{ nm}) = 1$, $B(4S, 497.2 \text{ nm}) = 0.574$, $B(4D, 460.3 \text{ nm}) = 0.77$, $B(5D, 413.3 \text{ nm}) = 0.76$, and $B(2P, 670.8 \text{ nm}) = 1$.

We assume that $K(\lambda)$ and $\Delta\Omega$ are independent of λ and divide Eq. (1) for $i = nS$ or nD by that for $i = 2P$ to obtain

$$\begin{aligned} \frac{Q_i(E)}{1 - \frac{1}{3} P_{i\lambda}} &= \frac{S(i, \lambda)}{B(i, \lambda) D(\lambda) T(\lambda)} \\ &\times \frac{B(2P, 6708) D(6708) T(6708)}{S(2P, 6708)} \\ &\times \frac{Q_{2P}(E)}{1 - \frac{1}{3} P_{6708}}. \end{aligned} \quad (2)$$

Here P_{6708} is the measured polarization of the 670.8-nm resonance line and Q_{2P} the total cross section, which we take from Ref. 3. Note that the presence of cascade contributions in the 670.8-nm line is taken into account by this procedure while the $Q_i(E)$ obtained from the data include cascading.

The S-state emission is unpolarized, so the measurements yield $Q_i(E)$ directly for this case. The resulting S-state total cross sections are labeled $nS + \text{CASC}(\text{Exp. } Q_T)$ in Figs. 2-5. (The low-energy behavior of the cross section is given

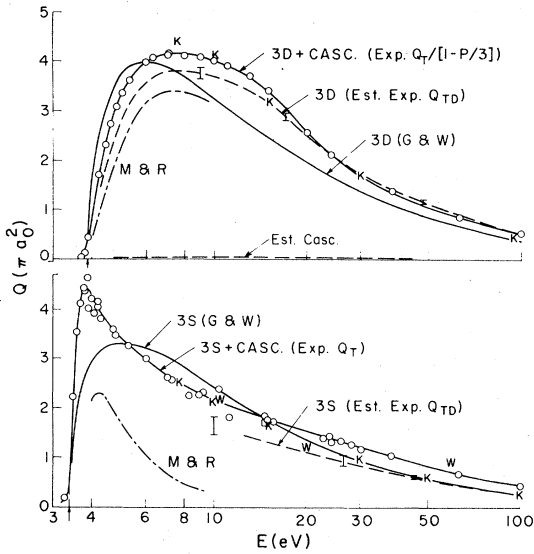


FIG. 2. Cross sections for excitation of the 3S and 3D states. The Born cross sections labeled G and W are from Greene and Williamson (Ref. 5), the K refer to points calculated by Korf (Ref. 8), the M and R curves are drawn through points calculated by McCavert and Rudge (Ref. 7) and the W points are measurements of the direct 3S cross section by Williams *et al.* (Ref. 10). The present experimental points are indicated as open circles, with an averaged line drawn through them. These data have been reduced to obtain an estimate of the total direct cross section, labeled "Estimated Experimental Q_{TD} ." The estimated cascading is indicated for the 3D case; it is the difference between (Exp. Q_T) and (Est. Exp. Q_{TD}) for the 3S case. The difference between the measured (Exp. $Q/[1-P/3]$) and (Est. Exp. Q_{TD}) for the 3D case is primarily due to an estimated polarization correction.

in Figs. 2 and 3, and the high-energy behavior in Figs. 4 and 5). The *D*-state emission is polarized, but we did not measure this polarization, since this would have required long integrations of these weak signals. Thus the experiment obtains $Q_i/(1-\frac{1}{3}P_{i\lambda})$, including cascading, for the *D* states. These are labeled $nD + \text{CASC}(\text{Exp. } Q/[1-P/3])$ or $nD + \text{CASC}(\text{Exp. } Q_T)$ in Figs. 2–5. Based on the behavior of Born cross sections in hydrogen and threshold-polarization arguments, with some additional decrease of polarization due to the resolved fine structure of Li, we expect the polarization of this $nD \rightarrow 3P$ line to be about +40% at threshold and to drop rapidly to about -30% for all energies above ~50 eV. Approximate total direct cross sections Q_{TD} for the *D* states, based on this polarization estimate and a minor cascade correction (indicated in the figures) are indicated as dashed lines labeled $nD(\text{Est. Exp. } Q_{TD})$ in Figs. 2–5. This polarization correction is about +10% at high energy and -10% at threshold and its ac-

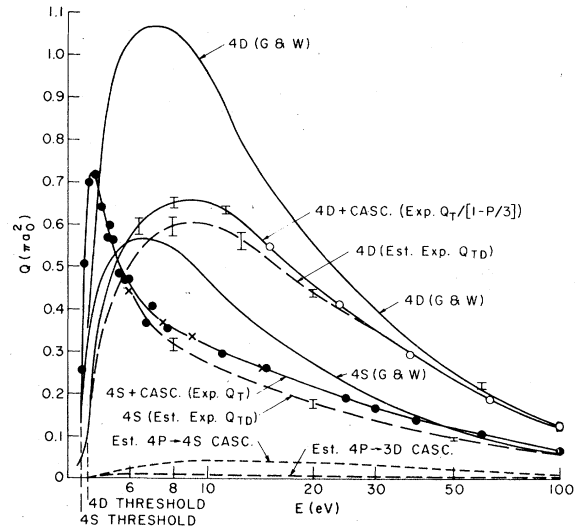


FIG. 3. Same as Fig. 2 for the 4S and 4D states.

curacy is probably a few percent. The estimated uncertainty in these corrected nD cross sections due to the scatter in the data plus cascade and polarization corrections is indicated as error bars in Figs. 2–5. The energy dependence of the 5*D*-state emission (413.3-nm) was also measured from 15–1200 eV and found to be the same as that for the 4*D* state; it is not shown in the figures.

We have utilized the Born cross sections of Ref. 5 to obtain the estimates of cascade corrections

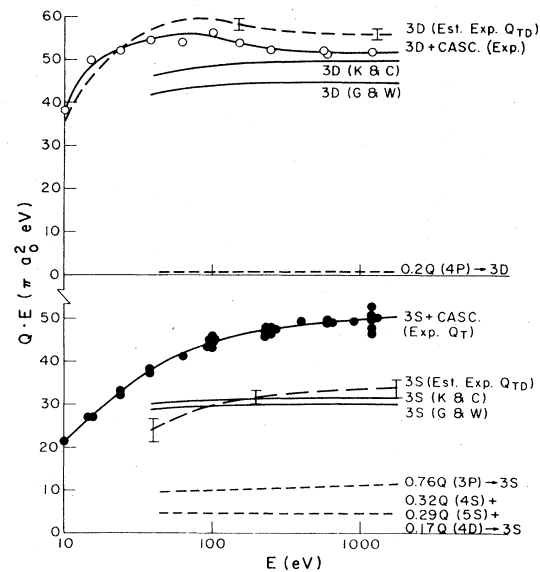


FIG. 4. Comparison of the high-energy behavior of QE , for the 3S and 3D states. The notation is the same as in Fig. 2, except that the entire Born cross sections, from Ref. 5, are used for the cascade contributions. The Born (K and C) refers to Ref. 6.

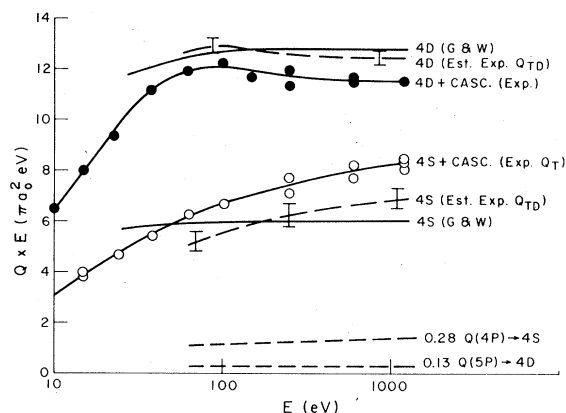


FIG. 5. Same as Fig. 4 for the 4S and 4D states.

given in Figs. 2–5. The branching ratios for these corrections are obtained from transition probabilities in Ref. 9. We have used the entire Born cross section for these cascade estimates above 50 eV, but a decreasing fraction of the Born cross sections for decreasing E below 50 eV. This is a minor distinction for the 3D and 4D states as the cascading is quite small. For the 4S states however, the uncertainty in this cascade-estimate results in $\sim 10\%$ uncertainty in Q_{TD} in the 8–30-eV region (Fig. 3). For the 3S state this uncertainty becomes so large that we have not continued the estimated Q_{TD} below ~ 12 eV (Fig. 2). The resulting uncertainties in Q_{TD} , plus that in the original data, are indicated as error bars in Figs. 2–5. These do not include the normalization uncertainty described at the beginning of this section.

COMPARISONS

There appear to be only two other measurements of excitation cross sections of the S and D states of Li. The first, by Aleksakhin and Zapesochnyi¹ in 1966, also obtained results for the resonance transition. That result was not reproduced in a later measurement by the same group, and they attribute² the discrepancy to errors in the earlier experiments, primarily due to secondary electrons. As this error would have been even more serious for the S- and D-state excitations that decrease more rapidly with increasing impact energy, we have not made quantitative comparisons with them here. However, their general behavior is consistent with the general pattern observed here; the S-state excitations have sharp peaks near threshold while the D states have broad peaks. The other measurement, by Williams *et al.*¹⁰ involved integration of the differential-energy-loss cross section, so that it is free of cascade contributions but can lose accuracy in the

extrapolation to zero-degree scattering. Of the states measured here only the 3S-state cross section was reported by Williams *et al.*; this is shown in Fig. 2, where it can be seen to be in reasonable agreement with our results except for the 60-eV point.

There have been many calculations of the Li 2P-state excitation cross section, but relatively few for the higher states. Two recent Born calculations provide interesting comparisons at the higher energies,^{5,6} and we are aware of two close-coupling calculations for lower energies.^{7,8} We have compared our results to the Born calculations at high energies in Figs. 4 and 5. For the 3S, 4S, 3D, and 4D states our results agree, typically within 10%, with these calculations at the highest energies. This supports the calculated cross sections as well as our assumption that using the manufacturer's photomultiplier quantum efficiency has introduced only (5–15)% experimental uncertainties. On the other hand, the magnitude of our 5D cross section (not shown) was only about 70% of the Born value, indicating that this relatively short wavelength (413.3 nm) was attenuated in the achromatic glass lenses of our detection optics.

The convergence to the high-energy (Born) limit, from above for the D states and from below for the S states, is quite interesting. There is an indication of this type of behavior in high-energy He-excitation data, which are compared to Born cross sections in Ref. 11. However, many of those measured cross sections do not converge to the Born values, or even to $Q \propto E^{-1}$.

It is rather surprising that the Born approximation is in fairly good agreement with the 3D cross section at all energies (Fig. 2). This may be fortuitous since the same calculation overestimates the peak of the 4D cross section by about a factor of 2 (Fig. 3). The estimated cascade contribution to the 3S cross section is a fairly large fraction of the observed Q_{Total} , so that the direct cross section Q_{TD} is rather uncertain. Nonetheless, it is apparent in Figs. 2 and 3 that the Born approximation overestimates the 3S and 4S cross sections in the 6–20-eV region by (30–50)% and it gives no indication of the sharp peak near threshold. We expect these lower-energy S- and D-state excitations to be strongly influenced by $2S \rightarrow 2P \rightarrow nS, nD$ coupling, which is neglected in the Born approximation.

We are aware of only two calculations of the low-energy behavior, aside from the Born calculation of Ref. 5, one by McCavert and Rudge⁷ and the other by Korf.⁸ Both utilize close coupling of the 2S, 2P, 3S, and 3D states plus additional approximations, and both obtain reasonably good

agreement with the measured $2P$ -state excitation cross section. Their results for the $3S$ and $3D$ states are shown in Fig. 2.

CONCLUSIONS

The measurements reported here demonstrate several interesting characteristics of the excitation cross sections for optically forbidden transitions. Some of these characteristics have also been observed in He excitation measurements, but they are much more clear and systematic in these Li cross sections. Foremost is the extremely different shape of the S - vs D -state cross sections, accompanied by the very similar shapes of the excitations to states differing in principal quantum number only. The smooth convergence to the Born cross sections at high energy is expected, but except for the resonance transitions this is the first demonstration of it. That this is so clear here, as opposed to the He case, is a result of the lower excitation energies in Li. As a consequence, the Li excitation cross sections are much larger, so that background and collisional effects are easier to eliminate.

The close-coupling calculations of Korf are impressively close to the experimental direct cross sections (dashed lines in Fig. 2) for these total excitation cross sections, in spite of his neglect of electron exchange. Unfortunately this agree-

ment does not explain why the cross sections behave as they do or what to expect for other species. Total scattering data of Johnston and Burrows¹² indicate that resonances occur just below the thresholds for exciting these states, and the rapid rise of the S -state excitation cross sections above threshold may be related to their presence. The present experiment indicates that the cross sections for states of different n are very similar once changes in excitation energy and magnitude are taken into account. Clearly, some simple scaling principles must be operative, as well as some differences between S and D states that do not depend on n . We do not yet have accurate data for $S \rightarrow S$ and $S \rightarrow D$ excitations in many other elements, but we have a strong suspicion that these characteristics are not specific to lithium and He. Just as with the resonance-line excitations⁴ some relatively universal behavior may be operative, so that major simplifications in the theory could be possible.

ACKNOWLEDGMENT

This work was supported in part by the National Science Foundation under Grant No. PHY76-04761 through the University of Colorado.

*Present address: Physics Dept., Amherst College, Amherst, Mass. 01002.

†Staff member, Quantum Physics Division, National Bureau of Standards.

¹S. Aleksakhin and I. P. Zapesochnyi, *Opt. Spektrosk.* **21**, 131 (1966) [*Opt. Spectrosc.* **21**, 77 (1966)].

²I. P. Zapesochnyi, E. N. Postui and I. S. Aleksakhin, *Zh. Eksp. Teor. Fiz.* **68**, 1724 (1975) [*Sov. Phys. JETP* **41**, 865 (1975)], see references therein.

³D. Leep and A. Gallagher, *Phys. Rev. A* **11**, 1082 (1974).

⁴S. T. Chen and A. Gallagher, *Phys. Rev. A* **17**, 551 (1978); E. A. Enemark and A. Gallagher, *ibid.* **6**, 192 (1972).

⁵T. J. Greene and W. Williamson Jr., *At. Data Nucl. Data*

Tables **14**, 161 (1974).

⁶Y. K. Kim and K. Cheng (private communication).

⁷P. McCavert and M. R. H. Rudge, *J. Phys. B* **5**, 508 (1972).

⁸D. F. Korf (private communication).

⁹W. L. Wiese, M. W. Smith, and B. M. Miles, *Atomic Transition Probabilities*, NSRDS-NBS No. 22 (U. S. GPO, Washington, D. C., 1969), Vol. II.

¹⁰W. Williams, S. Trajmar, and D. Bozinis, *J. Phys. B* **9**, 1529 (1976).

¹¹K. L. Bell and A. E. Kingston, *Adv. Atom. Mol. Phys.* **10**, 53 (1974).

¹²A. R. Johnston and P. D. Burrows, *Bull. Am. Phys. Soc.* **24**, 136 (1979).